

A hybrid microfluidic device for on-demand orientation and multidirectional imaging of *C. elegans* organs and neurons

Cite as: Biomicrofluidics **10**, 064111 (2016); <https://doi.org/10.1063/1.4971157>

Submitted: 23 July 2016 . Accepted: 16 November 2016 . Published Online: 02 December 2016

Ramtin Ardehshiri, Ben Mulcahy, Mei Zhen, and Pouya Rezai



View Online



Export Citation



CrossMark

ARTICLES YOU MAY BE INTERESTED IN

[A microfluidic device for automated, high-speed microinjection of *Caenorhabditis elegans*](#)
Biomicrofluidics **10**, 011912 (2016); <https://doi.org/10.1063/1.4941984>

[An automated microfluidic system for screening *Caenorhabditis elegans* behaviors using electrotaxis](#)

Biomicrofluidics **10**, 014117 (2016); <https://doi.org/10.1063/1.4941709>

[A perspective on optical developments in microfluidic platforms for *Caenorhabditis elegans* research](#)

Biomicrofluidics **8**, 011301 (2014); <https://doi.org/10.1063/1.4865167>



Biophysics Reviews

First Articles Now Online!

READ NOW >>>



A hybrid microfluidic device for on-demand orientation and multidirectional imaging of *C. elegans* organs and neurons

Ramtin Ardeshiri,¹ Ben Mulcahy,² Mei Zhen,^{2,3} and Pouya Rezai^{1,a)}

¹Department of Mechanical Engineering, York University, Toronto, Ontario M3J 1P3, Canada

²Lunenfeld-Tanenbaum Research Institute, Mount Sinai Hospital, Toronto, Ontario M5G 1X5, Canada

³Departments of Molecular Genetics and Physiology, University of Toronto, Toronto, Ontario M5S 1A8, Canada

(Received 23 July 2016; accepted 16 November 2016; published online 1 December 2016)

C. elegans is a well-known model organism in biology and neuroscience with a simple cellular (959 cells) and nervous (302 neurons) system and a relatively homologous (40%) genome to humans. Lateral and longitudinal manipulation of *C. elegans* to a favorable orientation is important in many applications such as neural and cellular imaging, laser ablation, microinjection, and electrophysiology. In this paper, we describe a micro-electro-fluidic device for on-demand manipulation of *C. elegans* and demonstrate its application in imaging of organs and neurons that cannot be visualized efficiently under natural orientation. To achieve this, we have used the electro-taxis technique to longitudinally orient the worm in a microchannel and then insert it into an orientation and imaging channel in which we integrated a rotatable glass capillary for orientation of the worm in any desired direction. The success rates of longitudinal and lateral orientations were 76% and 100%, respectively. We have demonstrated the application of our device in optical and fluorescent imaging of vulva, uterine-vulval cell (uv1), vulB1\2 (adult vulval toroid cells), and ventral nerve cord of wild-type and mutant worms. In comparison to existing methods, the developed technique is capable of orienting the worm at any desired angle and maintaining the orientation while providing access to the worm for potential post-manipulation assays. This versatile tool can be potentially used in various applications such as neurobehavioral imaging, neuronal ablation, microinjection, and electrophysiology. Published by AIP Publishing. [<http://dx.doi.org/10.1063/1.4971157>]

I. INTRODUCTION

Invertebrate organisms such as *Caenorhabditis elegans* (*C. elegans* or worm) and *Drosophila melanogaster* (*D. melanogaster* or fruit fly) are relatively homologous to humans in their genome¹⁻⁴ and have simple cellular and nervous systems. A wide variety of their mutants are available for biological investigations of human diseases and disorders.^{5,6} For instance, *C. elegans* is biologically simple (959 cells) and has a transparent body, which is an advantage for *in-vivo* microscopy. It has been successfully used as a model for studying toxin-induced degeneration of brain dopamine neurons in Parkinson's disease.^{7,8} Precise manipulation of the worm in desired longitudinal (anterior-posterior) and lateral (dorsal-ventral, left-right, or in between) orientations to access target cells, neurons, and organs of interest is important in various worm studies such as cellular and neural imaging,⁹ cell ablation,¹⁰ microinjection,¹¹ and electrophysiology.¹²

A freely crawling or swimming worm lies on its left or right side and moves longitudinally by propagating a dorsal-ventral bend along the anterior-posterior axis.¹³ Dorsal nerve cord (DNC), a tightly bundled neuropil that consists mostly of the axons and dendrites of motor

^{a)}Author to whom correspondence should be addressed. Electronic mail: prezai@yorku.ca. Tel: +1-416-736 2100 ext. 44703. Present address: BRG 433B, 4700 Keele St, Toronto, Ontario M3J 1P3, Canada.

neurons, runs along the length of the *C. elegans* body on the dorsal side. On one hand, lateral orientation to access the dorsal side is required for microinjection of needles into the gonad¹⁴ and for dissection of cuticle during electrophysiology.¹² On the other hand, ventral orientation (vulva facing the imaging system) is required for some multi-neuron imaging experiments (e.g., VC4/5 motor neurons) and egg-laying behavioral studies.⁹ However, the small size of *C. elegans* (50–70 μm diameter and 1 mm length in adult stage) and its continuous undulatory motion complicates the manipulation process and calls for development of tools and methods that are precise and easy to use for worm orientation.

Two conventional methods have been developed for *C. elegans* orientation, i.e., (i) maneuvering a single worm with a worm pick into an agar v-groove or (ii) spreading a population of worms over a flat agar surface and then placing a glass slide over the worms to maintain their random orientation. The former method is time-consuming and requires expertise to orient a single worm manually without damage, while the latter method requires a larger worm population to obtain an acceptable number of worms in the correct orientation. Despite its easiness and higher throughput, the oriented worms in the latter method remain inaccessible for post-orientation procedures such as chemical exposure, injection, or incision, which limits the use of this technique mostly to imaging applications.

Microfluidic devices are well-suited for manipulating and sorting^{15–17} of worms and have been developed for automated imaging and monitoring,^{18,19} behavioral screening,^{20–22} extracellular electrophysiological signal recording,^{23,24} and microinjection.^{25,26} Anterior-posterior orientation of the worm has been achieved by applying electric field in microchannels to cause electrotaxis response^{20,22,27} (100% head orientation towards the negative pole) or by the usage of micro-pillars²⁴ (71% longitudinal orientation) in microfluidic channels. However, lateral orientation has received less attention. Cáceres *et al.*²⁸ developed a novel U-shaped microfluidic channel to laterally orient *C. elegans* with 84% efficiency in the dorsal-ventral direction. The orientation enabled successful monitoring and sorting of different mutants based on their commissural neuron appearances at a high throughput. However, animals could be oriented dorsally or ventrally and the position of worms' ventral or dorsal side after orientation was random with 59% of worms' ventral side facing the inside of the U-channel. An acoustofluidic rotational manipulation (ARM) technique has recently been developed by Ahmed *et al.*²⁹ to investigate defective vulval morphologies in mutants by continuously rotating and imaging anesthetized worms in a microchannel. Microvortices generated by acoustically oscillating microbubbles have been used for this purpose. However, the use of anesthetized worms is not highly desired for biological investigations after orientation. Additionally, complete pressure equilibrium, proper transducer alignment on the chip, and trapped air bubbles were crucial to achieve controllable orientation which can impede further integration of this technique. There is a need for development of a more versatile and efficient tool for on-demand manipulation of non-anesthetized *C. elegans* in both longitudinal and lateral orientations while providing access to the worm after orientation for post-manipulation assays.

In this paper, we present a microfluidic device that is capable of selecting a single worm from a young adult population in a desired longitudinal direction and orienting it on-demand at any lateral direction. Longitudinal orientation from the head or tail side was achieved first by electrotaxis; then, the worm was laterally oriented in a microchannel trap by pneumatic capturing of its head or tail and manual rotation with an integrated glass capillary. A 3D-printed fixture enabled smooth and controllable rotation of the glass capillary inside the microfluidic device and hence orientation of the *C. elegans* at various lateral directions. The oriented worms could be fixed at any time in the device for post orientation assays. Our device empowers on-demand *C. elegans* orientation and can be applied to many similar small organisms such as zebrafish and fruit fly larvae with small changes to the design.

II. MATERIALS AND METHODS

A. Worm preparation

Wild type N2 strain worms were used in bright field imaging experiments. DY576: *him-8 (e1489); nIs96[Plin-11::GFP]*) and SGP14: *sgp1s7[F25B3.3::TagRFP,pJM24]* strains were

used for fluorescent imaging of *uv1* and *vulB1\2* cells as well as the ventral nerve cord (VNC). All experiments were performed using synchronized young adult worms at ambient temperature (approximately 22 °C). Gravid worms were initially washed from the Nematode Growth Medium (NGM) plate with M9 buffer (3 g KH_2PO_4 , 6 g Na_2HPO_4 , 5 g NaCl, and 1 ml 1M MgSO_4 in 1 l) and centrifuged for 1 min at 1200 rpm (revolutions per minute). Excessive liquid was removed, leaving behind the worm pellet. Worms were bleached (8.25 ml ddH_2O , 3.75 ml 1M NaOH, and 3.0 ml bleach) and hand shaken for 5 min and centrifuged for 1 min at 5000 rpm. Collected eggs were then washed three times with M9 for 1 min at 5000 rpm. Embryos were hatched and halted at the L1–L2 stage after 24 h post bleaching. The worms were then transferred onto a new NGM plate, and the growth was monitored until the L4 stage. Experiments took place 24 h post L4 stage on young adult animals. Prior to each experiment, worms were washed with M9 from the plate, centrifuged (1200 rpm), and washed 3 times to clean the sample.

B. Design and fabrication of the hybrid microfluidic device

The microfluidic chip (Fig. 1(a)) consisted of three major components, i.e., a single worm selection module, an orientation and imaging channel, and a rotatable glass capillary actuator shown in Fig. 1(b) at 5× magnification. The worm selection module was designed to enable loading of one worm at a time into the imaging channel. This module contained positive and wire electrodes inserted into the reservoirs of input and recirculation channels as well as a tapered microchannel (narrowing from 35 μm to 25 μm width) to trap a young adult worm from a synchronized population. The orientation and imaging channel included a 65 μm wide microchannel for lateral manipulation with side suction channels to immobilize the worm (480 μm total length). The rotatable glass capillary actuator was placed in front of the orientation and imaging channel and used to capture the head of the worm and rotate it until reaching the desired orientation. The glass capillaries (1B100-4, World Precision Instruments Inc., USA)

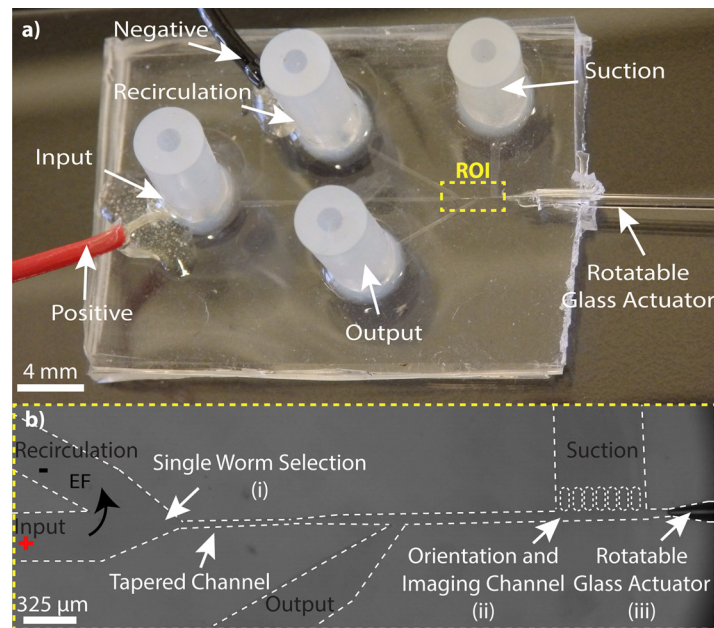


FIG. 1. (a) An overview of the hybrid microfluidic chip for *C. elegans* longitudinal and lateral orientation and imaging. (b) Region of Interest (ROI) of the microfluidic chip and its modules, i.e., (i) single worm selection, (ii) orientation and imaging channel, and (iii) rotatable glass capillary actuator. The channel height was 65 μm . The orientation and imaging channel was 65 μm wide (~ 10 – 15 μm larger than a young adult worm) and over 1 mm long with side suction channels implemented at its side for a total length of 480 μm .

were pulled by Sutter P-1000 (Sutter Instrument, USA) with the Bee-Stinger recipe³⁰ and were broken at the tip to provide 30 μm inner diameter (ID).

To fabricate the microfluidic device, a 2D design of the chip was sketched in AutoCAD (Autodesk Inc., USA). The sketched design was printed with a μPG501 chromium mask writer (Heidelberg GmbH, Germany) on a glass mask. A photoresist (SU8-2035 MircoChem, USA) was spun at 1400 rpm on a 3 in.-diameter silicon wafer, resulting in a 65 μm thickness. After soft baking (65 °C for 2 min and 95 °C for 8 min), the wafer was placed in a EVG 620 mask aligner (EV Group Inc., USA) with the printed mask on top, and exposed to the UV light (250 mJ/cm^2) in order to crosslink desired features on the wafer. Post-exposure bake (65 °C for 2 min and 95 °C for 7 min) was performed after UV exposure. Subsequently, the baked wafer was developed with SU-8 developer for approximately 7 min, rinsed with SU-8 developer and isopropyl alcohol (IPA), and dried with a N_2 gun to obtain the master mold. Feature sizes were measured with a Bruker optical profiler (Bruker Optics, USA). Polydimethylsiloxane (PDMS, Sylgard 184, Dow Corning Corp., USA) was used to produce a negative replica of the master mold. A 1 mm-diameter glass capillary was then fixed with half-cured PDMS on the master mold (at desired location) in order to serve as the housing for later-stage installation of the rotatable glass capillary. Subsequently, 10:1 ratio PDMS was poured over the master mold and cured for 3 h at 80 °C. After peeling off the cured PDMS layer, the template glass capillary was removed, and the rotatable glass capillary was installed into its respective location. This layer was then oxygen plasma bonded at 900 mTorr pressure and 50 W power for 30 s (PDC-001-HP Harrick Plasma, USA) to another flat PDMS layer.

C. Experimental setup

The described hybrid microfluidic device (Fig. 1) was used to select and load a single worm from a synchronized young adult worm population, then rotate and orient it at desired angles via rotating the glass capillary, and finally image it optically or fluorescently in the device. Fig. 2(a) shows the overall experimental setup used for on-demand orientation of *C. elegans*, which was necessary for the operation of the microfluidic device. The setup consisted of three main modules, i.e., a 3D-printed fixture to operate the hybrid microfluidic device, a sample manipulation module to control worms' orientation in the device, and image acquisition and analysis components.

One of the most important functions of the microfluidic chip was its ability to provide accurate rotation of the glass capillary inside the imaging channel to facilitate *C. elegans* orientation on the chip. For this, a fixture shown in Fig. 2(b) was designed and 3D-printed with a ProJet HD 3000 printer (3D Systems, USA). The 3D-printed fixture included a luer-lock holder, a glass capillary holder, and a space for positioning the microfluidic chip. The glass capillary holder (Fig. 2(c)) consisted of a movable v-groove plate, a spring housing to hold two springs, and a spring cap to secure the glass capillary by the springs. The microfluidic device was inserted into the 3D-printed fixture and the glass capillary was secured in the v-groove plate via the glass capillary holder to minimize its lateral and vertical movements. The glass capillary was then connected to a 1 ml syringe via a 0.8 mm silicone tube and two luer-lock connectors. This syringe was used for pneumatic capturing of the worm at the tip of the capillary using a negative suction force and also to apply manual rotation to the glass capillary and hence to the worm for orientation purposes. The luer-lock holder was used to secure the connectors attached to the syringe in place to prevent any axial movement artifacts to be delivered to the glass capillary in the device.

The sample manipulation module consisted of a syringe pump, a DC power supply, and a regulated lab-bench vacuum source controlled by a solenoid valve system. The syringe pump (Legato 110, KD Scientific Inc., USA) was used to deliver a population of synchronized worms into the input channel. The DC power supply (KEITHLEY 2636, Keithley Instruments Inc., USA) was used to apply a desired DC electric field for longitudinal (i.e., tail or head) orientation of the worms.^{20,27} The lab-bench vacuum source was regulated by a vacuum gauge (0–15 psi, Cole-Palmer, USA) and pulsed to the glass capillary actuator in the device by a

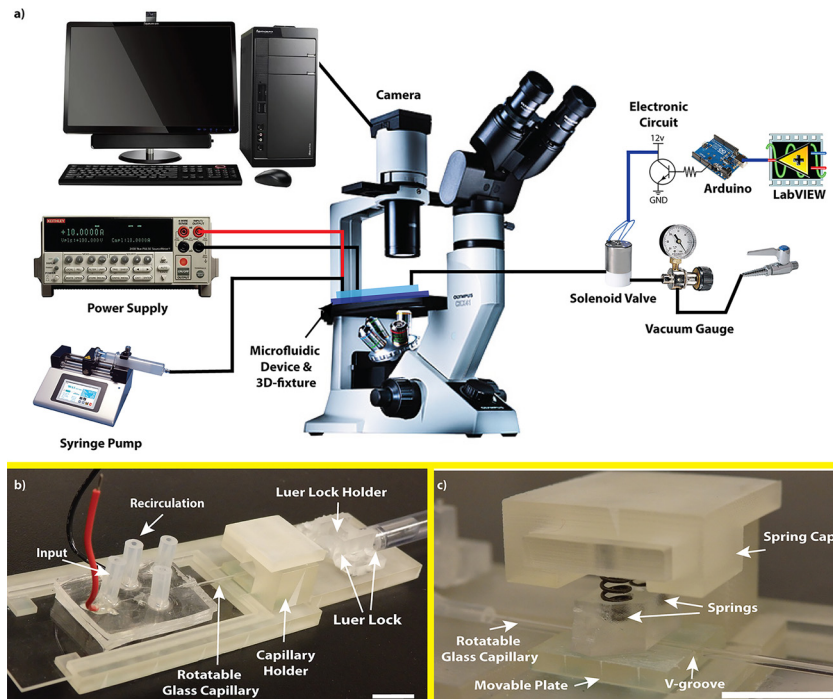


FIG. 2. (a) Experimental setup consisting of microscope, hybrid microfluidic device, 3D-printed fixture, DC power supply, solenoid valve, syringe pump, vacuum gauge, and electronic components. (b) 3D-printed fixture included a luer-lock holder, a glass capillary holder, and a space for positioning the microfluidic chip. (c) Glass capillary holder showing a movable plate containing a v-groove, the rotatable glass capillary, two springs, and a spring cap. Scale bars: 1 cm.

solenoid valve (3-Way direct lift solenoid valve (12 V), Cole-Palmer, USA). The operation of the solenoid valve was controlled by a microprocessor (Arduino Uno, Arduino LLC, Italy) and a simple electronic circuit (resistors and a NPN transistor) to provide 12 V pulsations. LabVIEW (National Instruments, USA) was used to control the microprocessor and to apply different waveform frequencies. Pulsed and regulated suction was applied through a 1/16th silicon tube which was press fitted to the end of the 1 ml syringe connected to the glass capillary. An inverted microscope (BIM-500FLD, Bioimager Inc., Canada) and a camera (GS3-U3-23S6M-C, Point Grey Research Inc., Canada) were used to capture bright-field and fluorescent images and videos of manipulated worms for further analysis using ImageJ software.

D. Experimental procedure

A synchronized population of young adult worms was delivered to the middle of the input channel using the syringe pump. The flow was stabilized and a 2.6 V/cm electrical field²⁰ (desired for young adults) was applied to the worms to instigate their longitudinal orientation towards the tapered worm selector channel. The direction of the electric field could easily be reversed (with a switch on the power supply) for tail loading purpose, which is not achievable reliably by other mechanical methods such as micro-pillars. The worms were then pushed towards the worm selector with various flow rates and possibility of trapping a single worm in the tapered channel while washing the rest of them out through the recirculation channel was investigated. After this step, the recirculation channel was closed in order to load the selected worm into the orientation and imaging channel. The effects of vacuum pressure magnitude and pulsation frequency on capturing the worm with the rotatable glass capillary were investigated for later-stage lateral manipulation and imaging. Images of manipulated worms were taken at 10 \times magnification for further dimensional analysis by ImageJ software. The percentage of worm body left outside of the glass capillary (inside the imaging channel) was used to

determine the best setting for pneumatic manipulation of worms. The selected setting was then used for lateral manipulation of three different strains of *C. elegans* in the chip and their multi-directional imaging. To demonstrate different orientations, bright field and fluorescent images (red and green) of different organs and neurons were obtained. The vulva in wild type worms is easily recognizable, lies on the ventral side of the worm, and can be used to determine different orientations in bright field images. VNC neurons were imaged in pan-neuronal RFP strain (SGP14) at different orientations. VNC was used for orientation demonstration as it contained 80% of neurons in comparison to 20% for dorsal nerve cord (DNC) and hence was seen as a single bright nerve cord along the ventral side of the worm. Further, the developed device enabled us to observe vulva cells (uv1 and vulB1\2) at three distinct orientations under 10 \times magnification in DY576 strain.

E. Chemotaxis assay

To investigate the effect of manipulating worms with the glass capillary, a chemotaxis assay (4 trials in triplicate, $N \approx 20$ worms per experiment) was performed off the chip to avoid the possibility of mixing treated worms with the untreated ones. A 200 μl suspension of worms was pipetted onto a Petri dish and placed under the microscope adjacent to the tip of a glass capillary connected to the regulated vacuum source. Worms were captured individually in a way that not more than 30% of their bodies were drawn into the glass capillary in 1 min (as practiced in the chip). After 1 min, pressure was turned off and worms were released into a M9 droplet. The captured worms were then transferred to a food race plate and placed 5 cm away from a 0.5 mm-diameter *Escherichia coli* (OP50) colony. Worms' movement towards the food colony was monitored for 2 h. Every 10 min, worms that reached the food colony were counted and discarded. At the end of 2 h, the remaining worms were counted to obtain the total number of worms. The same chemotaxis experiment was performed for parallel control groups which went through the same procedure without the glass capillary manipulation.

III. RESULTS AND DISCUSSIONS

The novel hybrid microfluidic device shown in Fig. 1 was developed to address the technological need in *C. elegans* studies requiring desired longitudinal and lateral orientation. It enables on-demand orientation and multi-directional imaging of organs and neurons with no need for anesthetizing the animals while providing post-orientation access to the worm. Operation of the device was facilitated by a custom-designed 3D-printed fixture and an experimental setup (Fig. 2) that are fully described in Section II. In this section, we characterize the performance of our device, investigate the effect of pneumatic capturing on worms' chemotaxis behavior, and demonstrate the application of our technique in multi-directional orientation and imaging of three *C. elegans* strains.

A. Rotation precision of the glass capillary in the hybrid microfluidic chip

Successful orientation of a worm inside our microfluidic chip depended strongly on smooth and stable rotation of the glass capillary inside the orientation and imaging channel. We determined that axial, lateral, and vertical displacements of the glass capillary tip during a full rotation should not have exceeded 30 μm inside the chip. This range was selected to prevent the glass capillary tip (OD $\approx 40 \mu\text{m}$) from contacting the channel walls that could result either in breakage or blockage by residual PDMS. In order to achieve improved precision in the glass capillary rotation and minimize its movements in the device, we designed and developed a 3D-printed fixture as shown in Figs. 2(b) and 2(c). This fixture eliminated the artifacts of the operator's hand during rotation and enabled smooth and controllable rotation of the glass capillary. Several design aspects were considered to achieve the 30 μm displacement resolution in the axial, lateral, and vertical directions. A commercially available luer-lock connector and a custom-designed holder on the fixture were used to minimize the axial movement of the flexible tubing, hence the glass capillary, during the manual rotation. This connector also facilitated

easy connection of the glass capillary to the external suction source that was used for manipulating the worms. The glass capillary was also passed through a v-groove plate in between the luer-lock holder and the microfluidic device that allowed minimizing its lateral displacement during the operation. The glass capillary was held inside the v-groove with the application of a vertical force via a top plate that was pushed against the capillary glass with a set of two compressed back-springs. The force exerted by the springs and the top plate was optimized to hold the glass capillary in the v-groove (eliminating vertical motions) while allowing its easy rotation for worm manipulation. To account for the height mismatch between the fixed glass capillary and the microfluidic channel in various devices, we precisely controlled the thickness of the bottom PDMS layer in the device (at ~ 3.7 mm) and incorporated a leveling screw in the fixture that allowed us to adjust the height of the v-groove plate at desired locations that corresponded precisely to each device. To demonstrate the necessity of the fixture, movement of the glass capillary tip inside the microfluidic device was measured in two different scenarios, i.e., with or without the 3D-printed fixture (Figs. 3(a) and 3(b), respectively). Three different devices were tested for each scenario, and the axial (ΔX) and lateral (ΔY) movements of the glass capillary tip were measured during 10 continuous rotations.

Results in Fig. 3(c) show a significant improvement in the lateral and axial displacement of the glass capillary tip inside the device when using the 3D-printed fixture to perform rotations. The average lateral and axial displacements reduced from $75 \mu\text{m}$ to $22 \mu\text{m}$ and from $48 \mu\text{m}$ to $7 \mu\text{m}$, respectively, demonstrating that the use of fixture was necessary for continuation of our experiments. The small movements at the tip can be attributed to the 3D-printer resolution to produce smooth and flat surfaces as well as possible excess forces that may have been applied

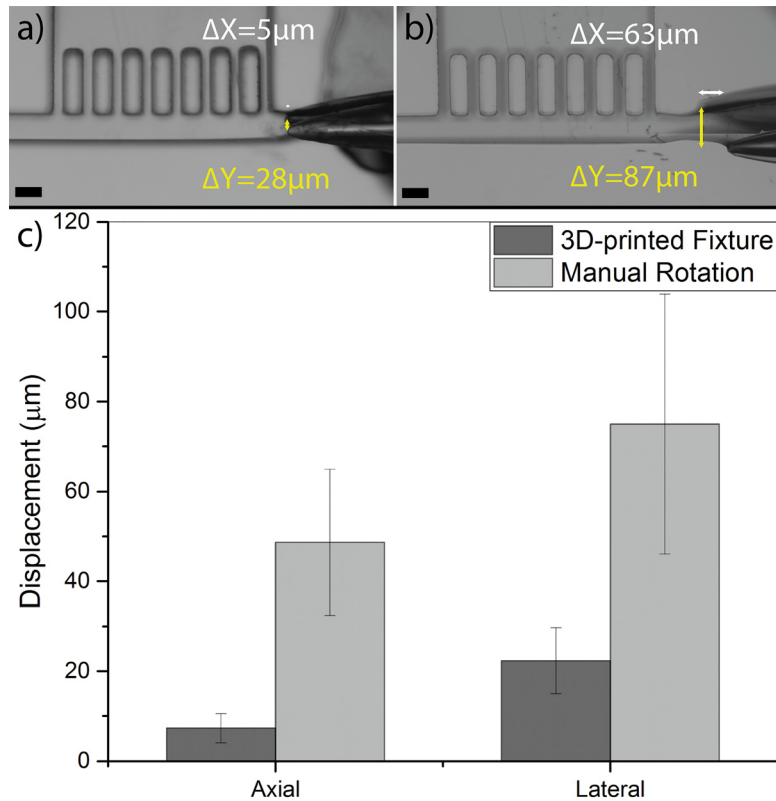


FIG. 3. Axial (ΔX shown by white bars) and lateral (ΔY shown by yellow bars) displacements of the glass capillary tip inside the microfluidic device, shown by overlapping all the capillary positions onto one image, when operated with (a) the 3D-printed fixture and (b) manually with no fixture. (c) Average and standard deviation of glass capillary tip displacement in lateral and axial directions when operated with 3D-printed fixture or manually inside $N = 3$ different devices. The scale bar is $65 \mu\text{m}$.

during the operation. However, we will show later that these capillary tip displacements were acceptable for achieving multi-directional orientation of worms, mainly due to flexibility of the worm and the distance of the imaging location (e.g., vulva) from the glass capillary tip.

B. Single worm selection with longitudinal orientation

The single worm selection module had two major roles to play in our device, i.e., (i) to orient worms longitudinally with heads (or tails, not shown in this paper) towards the orientation and imaging channel and (ii) to select and load one worm at a time from the synchronized worm population into the imaging channel. For longitudinal orientation of worms, we utilized the natural preference of *C. elegans* to move towards the negative pole when exposed to electric field (electrotaxis).^{20,27} For this experiment, a population of young adult worms was loaded into the inlet channel of our device. To determine the efficiency of electrotactic longitudinal orientation approach, loaded animals were exposed to 2.6 V/cm electric field (optimum for young adult animals²⁰) for 30 s after loading and then transferred with a 3 μ l/s flow rate towards the tapered microchannel at the entrance of the orientation and imaging channel. The longitudinal orientation of the worm that got trapped at the entrance of the tapered channel was then determined. A worm loaded with head was deemed as a successful longitudinal orientation. The results for head-loading are shown in Fig. 4 in comparison with a control group of animals that were not exposed to any electric field before loading into the tapered channel.

In the absence of electric field (WithoutEF group in Fig. 4), the longitudinal orientation of worms loaded into the tapered channel was random and resulted in an average success rate of 46% head orientation. But, in the presence of electric field (WithEF group in Fig. 4), the average success rate in head orientation was increased to 76% of the worms. This shows the effectiveness of electrotactic method in proper longitudinal orientation of worms and their anterior loading into the orientation and imaging channel. Bordertaxis (attraction to surfaces) and positive rheotaxis (alignment against fluid flow)³¹ can be the causes of tail loading that dominated orientation of worms not exposed to electric field but was overpowered by electrotaxis when an appropriate electric field was applied in the channel. It must be noted that as opposed to the existing mechanical methods for head orientation, the electrotaxis method provides the

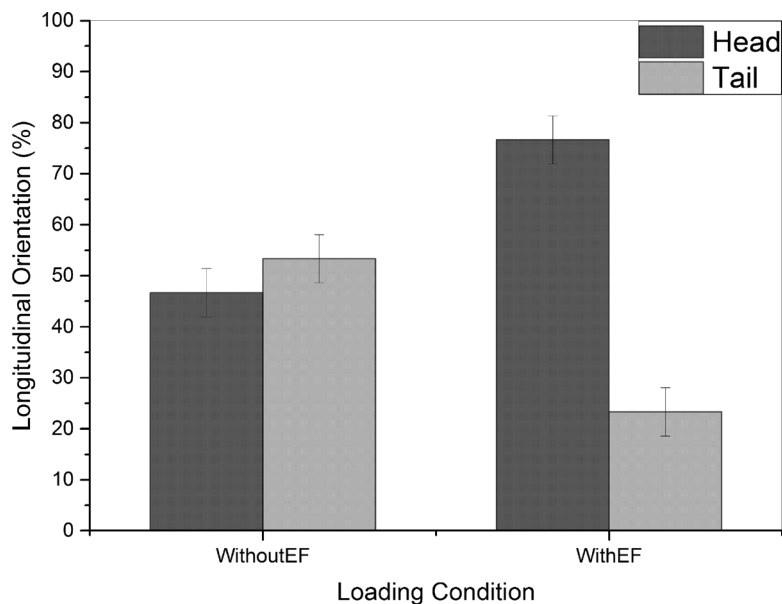


FIG. 4. Longitudinal orientation of worms loaded into the tapered channel in the absence of electric field (WithoutEF, N = 30 in 3 trials of 10 worms) or when the worms were exposed to electric field (WithEF, N = 30 in 3 trials of 10 worms). Electrically exposed worms showed an average of 76% head orientation after loading in comparison to 46% for the control group.

versatility of on-demand loading of worms with head or tail (not shown here) into the trap region of the device. This is important for multi-directional imaging of organs or cells that are located in the tail or head region of the worm, respectively, which was not the focus of this work.

After obtaining the desirable longitudinal orientation of a worm and loading it into the tip of the tapered channel (Fig. 5(a)), other remaining worms that had been loaded into the inlet channel were washed out of the device so that only the captured worm would be retained for lateral orientation and imaging. For this purpose, worms were washed out to the recirculation channel with a $1 \mu\text{l/s}$ flow of M9 buffer (Fig. 5(b)). The worm pre-loaded into the tapered channel however remained in the device because a hydrodynamic force was maintained at the back of the worm throughout the washing process. The recirculation channel was then closed (Fig. 5(c)) and the selected worm was loaded into the multidirectional orientation and imaging channel with a $3 \mu\text{l/s}$ flow of M9 buffer (Fig. 5(d)). The process of selecting a worm, washing the device, and transferring the selected worm to the orientation and imaging channel took an average of 75 s and yielded a success rate of approximately 77% for 30 animals tested.

C. Optimized setting for pneumatic capturing of *C. elegans*

The single worm selection module allowed the user to longitudinally orient a population of worms in the device and load only one of them into the orientation and imaging channel. We desired to pneumatically manipulate (i.e., capture the head and rotate) the selected worm in this channel for multidirectional imaging of organs and neurons. The rotatable glass capillary, positioned at the end of the orientation and imaging channel (Fig. 1(b)) and connected to the regulated and pulsed suction source, was used to capture the worm's head and orient it laterally in the device. The duration and magnitude of the applied pneumatic force played an important role in manipulation of worms and had to be assessed and optimized first. In order to determine the optimum operation condition, that allowed for capturing the head of the worm without pulling too much of its body into the capillary, the effect of vacuum pressure (5, 10, and 15 psi) and pulsation frequency (continuous, 5 Hz, and 15 Hz) applied to the capillary was investigated for a time duration of 1 min. The quality of manipulation was assessed by measuring the percentage of the worm's body remaining outside the glass capillary after 1 min of pneumatic actuation as shown in Fig. 6(a). Experiments were performed on $N=10$ animals at each actuation setting and the results are shown in Fig. 6(b).

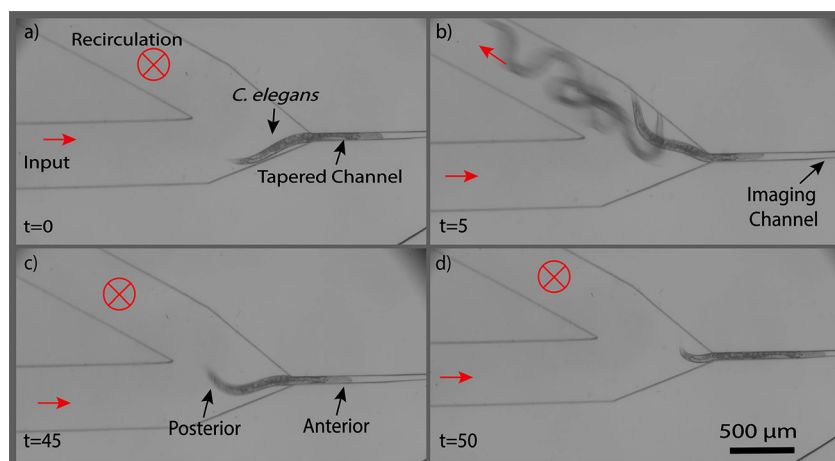


FIG. 5. Time-lapse images of single worm selection after electrostatic longitudinal orientation in the device. (a) Single worm loaded into the trap after longitudinal orientation, (b) recirculation channel was opened and rest of the worms were washed out, (c) recirculation channel was closed, and (d) selected worm was inserted into the imaging module. Times are in seconds and red arrows indicate the flow direction in the channel.

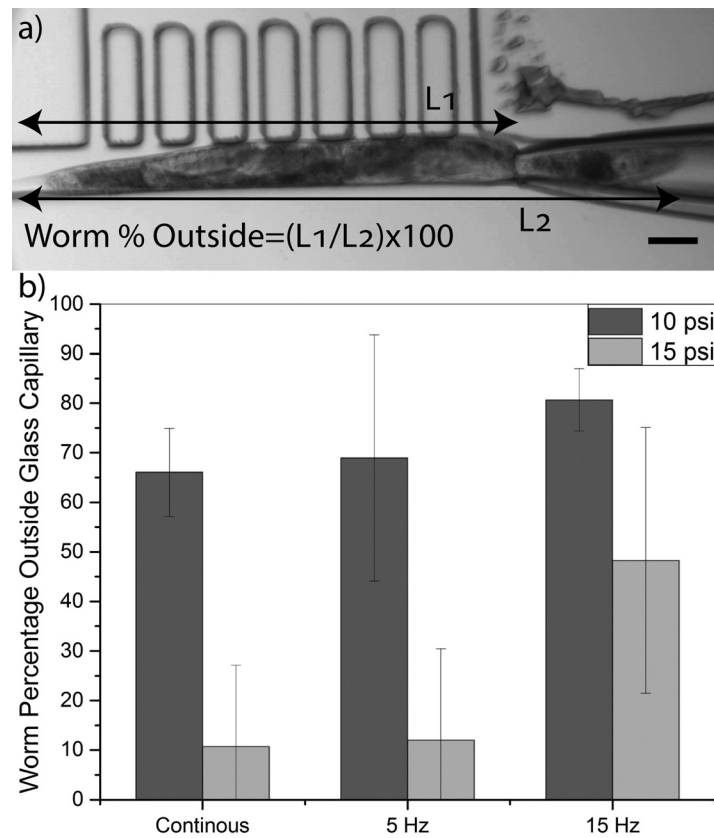


FIG. 6. (a) Image (10 \times) taken after 1 min pneumatic manipulation of a young adult worm at 10 psi pressure pulsated at 5 Hz frequency. Worm percentage outside of the glass capillary was calculated as $(L_1/L_2) \times 100$. (b) Worm percentages (average \pm S.E.M) outside the glass capillary manipulated with 10 and 15 psi vacuum pressures at different pulsation frequencies (continuous, 5 Hz, and 15 Hz) for 10 worms at each condition. The scale bar is 65 μ m.

A successful head capturing was defined as more than 70% of the worm's body being left outside the glass capillary after the 1-min pneumatic manipulation. When a 5 psi vacuum pressure was applied to the capillary, no matter what the pulsation frequency was, the captured worms were able to release their head from the glass capillary. Hence, manipulation was deemed unsuccessful at this pressure and not reported in Fig. 6(b). At 15 psi vacuum pressure, more than half of the body was pulled into the glass capillary at continuous pressurization or under 5 Hz pulsation. Increasing the frequency to 15 Hz led to higher percentage (48%) of worms' body to be outside of the glass capillary. However, this setting was still not desirable for our purpose. At 10 psi vacuum pressure, less percentage of worms' body was pulled inside the glass capillary when compared with other pressure settings. On average, continuous mode and 5 Hz pulsation at 10 psi resulted in 66% and 68% of worms' body being left outside of the glass capillary, respectively. By increasing the frequency to 15 Hz, the average percentage of worms' body outside the glass capillary increased to 80%. This optimized setting (10 psi and 15 Hz) was used for pneumatic manipulation of worms for lateral orientation and multidirectional imaging in the rest of our experiments.

D. Effect of pneumatic capturing on *C. elegans* chemotaxis

In order to investigate the effect of glass capillary capturing on worms' post-orientation behavior, the chemotaxis assay was performed as described in Section II. Approximately $N=240$ worms (in 4 triplicate trials) were captured for a minute with a glass capillary and then transferred to the food race plate. Fig. 7 shows the percentage of worms reaching the food colony at 10-min intervals for the manipulated (with pneumatic capillary) and control worms.

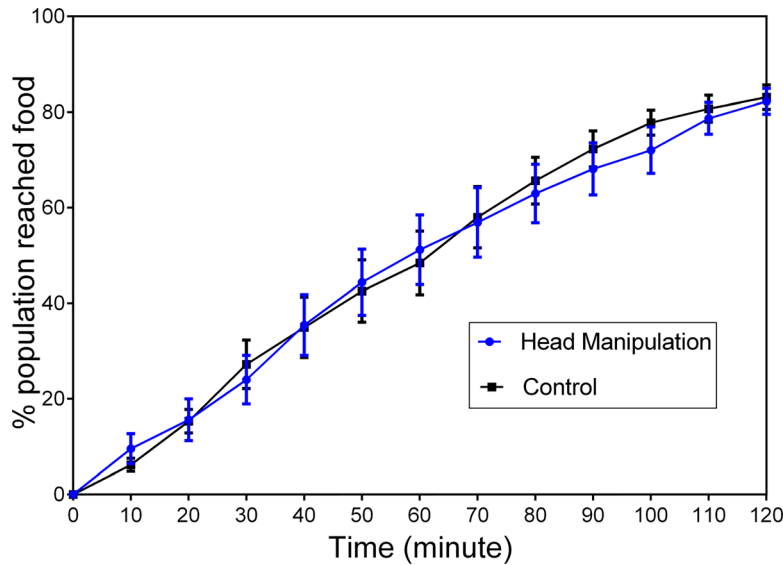


FIG. 7. Chemotaxis assay (error bars showing S.E.M) for the worms that were captured pneumatically with a glass capillary for 1 min (blue) in comparison to the control worms that were not manipulated with the capillary glass (black). Experiment was performed in four trials, each in triplicate of approximately $N = 20$ worms. No significant difference was observed between the manipulated and control groups (two-way ANOVA test, $P > 0.5$)

No significant difference was observed between the two groups of worms, indicating that pneumatic capturing had no effect on the worms' chemotaxis behavior when desirable pressure and pulsation conditions were applied. Our qualitative investigation of manipulated worms also demonstrated no visible effect on the egg-laying behavior; however, we recommend a quantitative analysis of this biological process and viability of the worms if the method is to be used for long-term off-spring investigations.

E. Multi-directional orientation of *C. elegans* for imaging of organs and neurons

We used our device to image neurons (ventral nerve cord or VNC) and vulva muscles (uv1 & vulB1\2) of young adult *C. elegans* at different orientations as procedurally discussed in Section II. To be able to orient an unanesthetized and freely moving worm that had already been selected from a population (Fig. 5), the optimized setting for pneumatic head manipulation by the glass capillary (i.e., 10 psi pressure pulsed at 15 Hz) was employed. Manual rotation applied through the 3D-printed fixture (Fig. 2) provided controllable rotation of the capillary at only one degree of freedom. The worm was captured and rotated on-demand until reaching the desired orientation for imaging. For demonstration purposes, images of a young adult worm were taken at three distinct orientations with 90° intervals as shown in Fig. 8 (Multimedia View). Both lateral (Figs. 8(a-i) and 8(a-iii)) and dorso-ventral (Fig. 8(a-ii)) orientations could be achieved conveniently. Typically, in a bright field image, the pharynx, gonads, and vulva of the worm are distinguishable organs, which may be used as landmarks for determining different orientations. For example, as in Figs. 8(a-i) and 8(a-iii), the lateral orientations of the worm were determined in reference to the side of the vulva (area directed by the red arrow). Vulva appears as an opening in the dorso-ventral orientation as shown in Fig. 8(a-ii). To further validate the dorso-ventral orientation, the pharynx terminal bulb can also be utilized.

Upon successful demonstration of wild type strain orientation in the bright field mode, two other strains were used for fluorescent imaging of ventral and dorsal cord neurons, as well as vulval muscle cells. A strain expressing RFP in all neurons (pan-neuronal RFP) was imaged as described above and various orientations are shown in Fig. 8(b). The VNC contains a larger bundle of neurites than the dorsal nerve cord (DNC); therefore, the VNC can be distinguished from the DNC based on the relative intensity of fluorescence. In addition to pan-neuronal

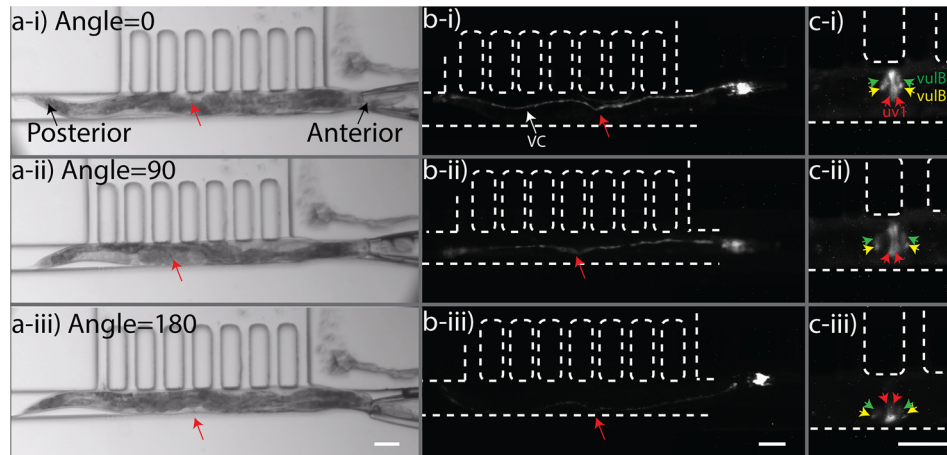


FIG. 8. (a) Young adult worm bright field images at 90° intervals: (i) lateral orientation (ventral side facing the suction channels), (ii) dorso-ventral orientation (ventral side facing the imaging system), and (iii) lateral orientation (ventral side facing the channel wall). Red arrows indicate the vulva. (b) RFP images of SGP14(*sgpIs7*) strain at 90° rotation intervals. Red arrows indicate the vulva. Ventral cord (VC) is shown with the white arrow in b-i. (c) GFP images of DY576 (*lin-11::gfp*) strain at 90° rotation intervals. Red arrows indicate *uv1* cells. Green and yellow arrows indicate *vulB1* and *vulB2* respectively. All scale bars are $65\ \mu\text{m}$. Movie 1 shows a full rotation of the *C. elegans* under 10 psi pressure and 15 Hz pulsation inside the microfluidic device. (Multimedia view) [URL: <http://dx.doi.org/10.1063/1.4971157.1>]

imaging, we could also use our device to acquire Green Fluorescent Protein (GFP) images of specific vulva muscle cells (*uv1* & *vulB1\2*) as shown in Fig. 8(c). The *uv1* muscle cells were clearly visible at dorso-ventral orientation in comparison to two other lateral orientations. The *VulB1\2* cells were distinguishable in all orientations with better spatial resolution in dorso-ventral orientation.

With the optimized setting in our device, we were able to orient 30 freely moving animals with a 100% success rate while being able to pause orientation at any desired time and direction for imaging of organs and neurons as demonstrated in Fig. 8. Previously developed orientation techniques^{29,32} can also manipulate worms in desired orientations; however, they require the worms to be chemically anesthetized. Chemical immobilization should preferably be avoided because anesthetics may have negative or inhibitory effects on worms' neuronal or behavioral processes that are sought in many applications. Our device could achieve active and on-demand orientation without the need for anesthetization but this was at the expense of reducing the throughput of experiments (20–30 worms per hour) to account for voluntary movement and escape of worms as well as manual imaging by the operator. Another novel U-channel microfluidic passive orientation technique²⁸ could orient unanesthetized worms with a higher throughput; however, orientation was only reported in the lateral direction. Our technique can orient unanesthetized worms at any desired orientation for further processing such as time-lapse chemical screening (to be investigated).

IV. CONCLUSION

We have developed a hybrid microfluidic device to orient *C. elegans* at any desired longitudinal and lateral angle for imaging of organs, neurons, and cells. Worms could be laterally oriented with 76% success rate using their inherent electro taxis response and then pneumatically captured with a glass capillary integrated inside the microfluidic device and orientated with 100% success in a narrow microchannel. A 3D-printed fixture was custom-designed to hold the microfluidic device and the glass capillary relatively fixed to each other, resulting in a smooth rotation of the capillary with lateral and axial displacement resolutions of $22\ \mu\text{m}$ and $7\ \mu\text{m}$. The pneumatic capturing process was optimized in the device at 10 psi pressure pulsed at 15 Hz to prevent applying excessive forces to the worms. A chemotaxis assay on the captured worms demonstrated that this process does not negatively affect the behavior of worms in

comparison to the ones that were not mechanically manipulated. Using the optimized manipulation settings, optical and fluorescent images of vulva and ventral cord as well as uv1, vulB1, and vulB2 cells could be successfully obtained with our device. Our hybrid microfluidic device will facilitate investigating the cells and neurons of unanesthetized worms at any desired orientation, in comparison to previously reported orientation techniques which required anesthetized worms and were complex to provide post-orientation access to animals. In its current configuration, our device is ideal for chemical screening and monitoring of various biological processes in naturally inaccessible cells, neurons, and organs of unanesthetized *C. elegans*. With design modifications, it can also be used in microinjection, electrophysiology, and laser ablation applications. The angular resolution of orientation in our device can be significantly improved upon motorization of the glass capillary rotation in our device. Moreover, the overall throughput of the device can be significantly increased by computerizing processes such as selecting, capturing, orienting, and releasing of the worm. This was not the focus of our work as we wanted to provide a semi-manual tool for adoption by the end users, but will be pursued in the next phase of the research to develop a fully automated version of this microfluidic multi-directional worm orientation device.

ACKNOWLEDGMENTS

This research was financially supported by the Natural Sciences and Engineering Research Council of Canada. The authors would like to thank Professor B. P. Gupta from McMaster University for providing the DY576 strain along with biological insights for vulva muscle imaging of *C. elegans*.

- ¹D. L. Riddle, T. Blumenthal, B. J. Meyer, and J. R. Priess, *C. Elegans II* (Cold Spring Harbor Laboratory Press, Cold Spring Harbor, NY, 1997).
- ²L. T. Reiter, L. Potocki, S. Chien, M. Gribskov, and E. Bier, *Genome Res.* **11**(6), 1114 (2001).
- ³E. Braungart, M. Gerlach, P. Riederer, R. Baumeister, and M. C. Hoener, *Neurodegener. Dis.* **1**, 175 (2004).
- ⁴M. Markaki and N. Tavernarakis, *Biotechnol. J.* **5**, 1261 (2010).
- ⁵T. Kaletta and M. O. Hengartner, *Nat. Rev. Drug Discov.* **5**, 387 (2006).
- ⁶U. B. Pandey and C. D. Nichols, *Drug Deliv.* **63**, 411 (2011).
- ⁷S. Salam, A. Ansari, S. Amon, P. Rezai, P. R. Selvaganapathy, R. K. Mishra, and B. P. Gupta, *Worm* **2**, e24558 (2013).
- ⁸R. Nass, D. H. Hall, D. M. Miller, and R. D. Blakely, *Proc. Natl. Acad. Sci. U.S.A.* **99**, 3264 (2002).
- ⁹M. Zhang, S. H. Chung, C. Fang-Yen, C. Craig, R. A. Kerr, H. Suzuki, A. D. T. Samuel, E. Mazur, and W. R. Schafer, *Curr. Biol.* **18**, 1445 (2008).
- ¹⁰S. H. Chung and E. Mazur, *Appl. Phys. A* **96**, 335 (2009).
- ¹¹C. C. Mello, J. M. Kramer, D. Stinchcomb, and V. Ambros, *EMBO J.* **10**, 3959 (1991).
- ¹²M. B. Goodman, T. H. Lindsay, S. R. Lockery, and J. E. Richmond, *Methods Cell Biol.* **107**, 409 (2012).
- ¹³J. T. Pierce-Shimomura, B. L. Chen, J. J. Mun, R. Ho, R. Sarkis, and S. L. McIntire, *Proc. Natl. Acad. Sci. U.S.A.* **105**, 20982 (2008).
- ¹⁴T. Evans, editor, "Transformation and microinjection" (April 6, 2006), *WormBook*, edited by The *C. elegans* Research Community, WormBook, <http://www.wormbook.org>.
- ¹⁵B. Han, D. Kim, U. H. Ko, J. H. Shin, U. Hyun Ko, and J. H. Shin, *Lab Chip* **12**, 4128 (2012).
- ¹⁶C. B. Rohde, F. Zeng, R. Gonzalez-Rubio, M. Angel, and M. F. Yanik, *Proc. Natl. Acad. Sci. U.S.A.* **104**, 13891 (2007).
- ¹⁷X. Ai, W. Zhuo, Q. Liang, P. T. McGrath, and H. Lu, *Lab Chip* **14**, 1746 (2014).
- ¹⁸W. Shi, H. Wen, B. Lin, and J. Qin, *Microfluidics* **304**, 323 (2011).
- ¹⁹S. E. Hulme, S. S. Shevkoplyas, A. P. McGuigan, J. Apfeld, W. Fontana, and G. M. Whitesides, *Lab Chip* **10**, 589 (2010).
- ²⁰P. Rezai, A. Siddiqui, P. R. Selvaganapathy, and B. P. Gupta, *Lab Chip* **10**, 220 (2010).
- ²¹P. Rezai, A. Siddiqui, P. R. Selvaganapathy, and B. P. Gupta, *Appl. Phys. Lett.* **96**, 153702 (2010).
- ²²P. Rezai, S. Salam, P. R. Selvaganapathy, and B. P. Gupta, *Biomicrofluidics* **5**, 44116 (2011).
- ²³S. R. Lockery, S. E. Hulme, W. M. Roberts, K. J. Robinson, A. Laromaine, T. H. Lindsay, G. M. Whitesides, and J. C. Weeks, *Lab Chip* **12**, 2211 (2012).
- ²⁴C. Hu, J. Dillon, J. Kearns, C. Murray, V. O'Connor, L. Holden-Dye, and H. Morgan, *PLoS One* **8**, e64297 (2013).
- ²⁵X. Zhao, F. Xu, L. Tang, W. Du, X. Feng, and B. Liu, *Biosens. Bioelectron.* **50**, 28 (2013).
- ²⁶P. Song, X. Dong, and X. Liu, *Biomicrofluidics* **10**, 11912 (2016).
- ²⁷J. Tong, P. Rezai, S. Salam, P. R. Selvaganapathy, and B. P. Gupta, *J. Vis. Exp.* **75**, e50226 (2013).
- ²⁸I. D. C. Cáceres, N. Valmas, M. A. Hilliard, and H. Lu, *PLoS One* **7**, e35037 (2012).
- ²⁹D. Ahmed, A. Ozcelik, N. Bojanala, N. Nama, A. Upadhyay, Y. Chen, W. Hanna-Rose, and T. J. Huang, *Nat. Commun.* **7**, 11085 (2016).
- ³⁰P.-M. Pullers, *Pipette Cookbook 2015 (P-97 & P-1000 Micropipette Pullers)*, Rev. E (Sutter Instrument Company, 2015).
- ³¹J. Yuan, D. M. Raizen, and H. H. Bau, *Proc. Natl. Acad. Sci. U.S.A.* **112**, 3158 (2015).
- ³²M. Rieckher, U. J. Birk, H. Meyer, J. Ripoll, and N. Tavernarakis, *PLoS One* **6**, e18963 (2011).